A data assimilation approach for estimating strength of steel pipes reinforced with composite sleeves under unsteady pressure-flow conditions

MACIEJ WITEK*
FERDINAND UILHOORN

Warsaw University of Technology, Plac Politechniki 1,00-661 Warszawa, Poland

Abstract The aim of this paper is twofold: to estimate the unsteady pressure-flow variations in gas transmission pipelines using the ensemble-based data assimilation approach and to analyse the strength of steel tubes reinforced with composite sleeves containing localized part-wall thickness loss caused by corrosion while taking into consideration a safe operating pressure of the pipeline. For a steel thin-walled cylinder containing a part-wall metal loss, a flexible wrap of fibreglass as well as carbon glass with epoxy resin are determined. The strength of the repaired pipeline with two kinds of materials for sleeves is investigated taking into consideration the internal pressure at the defect location. For the case study, a section of the Yamal transit pipeline on the Polish territory is selected. The results enable pipeline operators to evaluate the strength of corroded steel pipelines and develop optimal repair activities, which are of vital importance for the maintenance and operation of underground steel networks.

Keywords: Pipe wall metal loss; Composite sleeve; Pipe fracture; Gas dynamics; Data assimilation

Nomenclature

A – cross-sectional area of pipe, m^2
a_s – isentropic wave speed, m/s
c_p – specific heat at constant pressure, J/(kg·K)
d – defect depth derived from diagnostics, mm
D_i – interior pipe diameter, m
D_o – pipe diameter, m
E_{sleeve} – elasticity modulus in the circumferential direction of the composite sleeve material, GPa
E_{pipe} – elasticity modulus of steel, GPa
f – pipeline design factor, –
f_u – ultimate tensile strength of the pipe steel, MPa
f_y – yield stress of the pipe steel, MPa
f_r – friction factor, –
g – gravitational acceleration, m/s^2
L – defect length, mm
` – pipeline length, m
MAOP – maximum admissible operating pressure, MPa
$\dot{m}$ – mass flow rate, kg/s
n_k – measurement noise vector, Pa, K and kg/s
N_p – number of particles, –
p – pressure, Pa
p_{thmax} – failure pressure of a pipe with a volumetric defect reinforced a composite wrap, MPa
$p(x)_{est}$ – pressure estimated from the flow model at the metal loss coordinate x along the pipeline, MPa
R – specific gas constant, J/kg
Re – Reynolds number, –
r_e – external radius of the steel tube plus thickness of the sleeve, mm
r_i – inner radius of the steel pipe, mm
r_o – external radius of the steel pipe, mm
T – temperature, K
t – time, s

U – total heat transfer coefficient, $W/m^2 \cdot K$
v – velocity, m/s
v_k – model noise vector in time step k, Pa, K and kg/s
x – distance along pipeline, m
y_k – measurement vector in time step k, Pa, K and kg/s
z – compressibility factor, –
Δx – spatial step size, m

Greek symbols

δ – pipe wall nominal thickness, mm
ε – pipe roughness, m
ω_r – frictional force per unit length of pipe, N/m
Ω – heat flow, J/(m s)

π – probability density, Pa^{-1}, K^{-1} and $(kg/s)^{-1}$
ρ – density, kg/m^3
θ – angle of inclination, degrees
ζ_k – vector with state variables in time step k, Pa, K and kg/s

Subscripts

k – time
0 – initial
s – soil

Abbreviations

GERG – Groupe Européen de Recherches Gazières

1 Introduction

The most effective and widespread in-line inspection method for long-distance high-pressure underground pipelines is the so-called magnetic flux leakage (MFL) technology using axial excitation of magnetic field lines [1]. The data from MFL inspection gives insight into tube wall losses along the pipeline. This kind of defect assessment after periodic diagnostics is crucial in safe operation of natural gas grids [2]. It allows pipeline operators to evaluate the severity of flaws and to identify the anomalies that need to be repaired with composite sleeves. In [3], a three-step methodology was considered as a useful tool for operators to evaluate the severity of part-wall metal losses and the aging process of underground steel pipelines transporting natural gas. The time-dependent reliability of corroded steel pipelines with correlations of random variables and taking into consideration field-measured/direct-assessed defects dimensions, was presented in [4] as the application to different in-service buried pipelines in Canada.

Information concerning the internal pressure conditions is of utmost importance in estimating the structural integrity of tubes. In [5], pressure variations were estimated assuming steady-state flow conditions and the results were used to calculate the main load on the pipe wall. However, this approach is valid if the system does not undergo significant changes in the flow and pressure. In the present research, the unsteady gas pressure-flow conditions are considered while the fluid transients are realization of a stochastic process. Flow models are incomplete and contain uncertain-ties related to initial and boundary conditions, fluctuations in natural gas composition, surrounding temperatures, soil properties, etc. Therefore, the pressure, temperature and flow rate estimates might differ significantly

from reality. To solve this problem, an ensemble-based data assimilation approach, that is, particle filtering, is implemented [6–8]. It shows intriguing convergence properties and provides a framework for solving estimation problems not limited to linearity and Gaussianity.

The aim of this study is to use internal pressure estimates obtained from data assimilation. Sensitivity of the model noise parameters that represent the inexactness and uncertainties in the pressure-flow conditions model, compared to the previous study [22], is investigated. The choice of these parameters is of utmost importance because, if wrongly selected, divergence of the data assimilation algorithm may occur. Besides this new aspect, also two other kinds of commercially available flexible wraps are compared, in terms of a number of layers, in order to resist the internal pressure derived from an unsteady gas flow model, at a given defect location in the pipeline. The authors consider different materials for composite sleeves using fibreglass as well as carbon glass with epoxy resin to reinforce part-wall metal losses of underground steel pipelines, obtained from magnetic flux leakage inspections tools.

A decrease in the tube wall thickness caused by electrochemical corrosion is analysed considering the limit state of plastic rupture and the corresponding maximum operating pressure of the remaining pipe wall residual thickness. This value was compared to the estimated internal pressure obtained from the data assimilation approach at the point of the localized defect. The thickness of both sleeves, i.e. multi-layer fibreglass and carbon fibre ones was determined in order to reach the required strength of the pipeline. The bending moment was not taken into consideration. Fracture mechanics and material properties of steel pipelines repaired with composite sleeves have been extensively analysed in recent years using experimental and numerical approaches, e.g. in [24, 26]. Flexible wrap repair systems, in the form of overwrapping the steel pipes even at bends, are intensively used by the industry for onshore repairs for a wide range of pressure equip-ment applications. In recent years, composite repairs have been also used for offshore pipelines [23, 25].

Structural integrity receives plenty of interest due to its practical applications in oil and gas steel pipelines [5, 9]. A crucial component of in-service pipelines is to predict the probability of burst of the structure considering the maximum internal pressure as well as to implement the repair activities and for this reason the subject of this paper was selected. This research en-ables network operators of steel pipelines subjected to corrosion to handle capacity limitations based on transient pressure calculations.

2 Unsteady gas flow model

The governing equations describing the unsteady gas flow dynamics in pipeline systems are derived from the conservation principles of mass, mo-mentum, and energy. The set of partial differential equations (PDEs) can be formulated as follows [10]:

$$\frac{\partial w}{\partial t} + F(w)\frac{\partial w}{\partial x} + S(w) = 0, \quad \forall x \in R,\ t \in R^{+}, \tag{1}$$

where: $w = \begin{bmatrix} p & \dot{m} & T \end{bmatrix}$ and

$$F(w) = \begin{bmatrix} -\dfrac{Ap}{\dot{m}\,a_s^2\,\alpha_2 - RTz} & \dfrac{A}{a_s^2} & \dfrac{AT}{a_s^2 \dot{m} \alpha_1} \\ A - \dfrac{a_s^2\alpha_2^2 c_p \dot{m}^2 - R a_s^2 \alpha_1^2 \alpha_2 \dot{m}^2 z}{A c_p p^2} & \dfrac{\dot{m}}{A} \dfrac{\alpha_2 c_p a_s^2 - R z a_s^2 \alpha_1^2 + RT c_p z}{c_p p} & \dfrac{a_s^2 \alpha_1 \dot{m}^2}{AT c_p p} \dfrac{\alpha_2 c_p - R\alpha_1^2 z}{} \\ \dfrac{RT a_s \alpha_1 \alpha_2 m z}{} & \dfrac{RT a_s \alpha_1 z}{} & \dfrac{Rmz}{} \dfrac{a_s^2}{} \dfrac{\alpha_1^2}{} + T c_p \end{bmatrix}, \tag{2}$$

$$S(w) = \begin{bmatrix} -\dfrac{a^2 \alpha_1 (\Omega A p + RT \dot{m} \omega_r z)}{A^2 T c_p p} \\ \dfrac{}{} \dfrac{}{} \sin\theta \\ -\dfrac{a_s^2 \alpha_2 (\Omega A p + RT \dot{m} \omega_r z)}{A^2 c_p p^2} \end{bmatrix}, \tag{3}$$

where: T – temperature, p – pressure, $\dot{m}$ – mass flow rate, ω_r – frictional force, g – gravitational acceleration, A – cross-sectional area, θ – angle of inclination, Ω – rate of heat transfer, R – specific gas constant, z – compress-ibility factor and c_p – specific heat at constant pressure. The parameters α_1 and α_2 are defined as follows:

$$\alpha_1 = 1 + \frac{T}{z}\frac{\partial z}{\partial T}_p, \qquad \alpha_2 = 1 - \frac{p}{z}\frac{\partial z}{\partial p}_T. \tag{4}$$

The isentropic wave speed $a_s = (\partial p/\partial \rho)_s^{1/2}$ is calculated from the following expression:

$$\frac{\partial p}{} = \frac{\rho}{} \left(1 \frac{p}{} \frac{\partial z}{} T - \frac{p}{} \left(1 + \frac{T}{} \frac{\partial z}{}\right)^2 - 1\right), \tag{5}$$

where ρ is the density. The frictional force per unit length is defined as $\omega_r = \frac{1}{8} f_r \rho v|v| \pi D_i$ where v is the velocity and D_i is the internal diameter. The Colebrook-White equation is used to compute the friction factor, f_r [11],

$$\frac{1}{\sqrt{f_r}} = -2 \log \left(\frac{\varepsilon}{3.7 D_i} + \frac{2.51}{\mathrm{Re}\sqrt{f_r}} \right), \tag{6}$$

where ε denotes the pipe roughness and Re refers to the Reynolds number. The steady heat transfer between the natural gas and soil per unit length and time is defined as

$$\Omega = -\pi D_i U (T - T_S), \tag{7}$$

where U is the total heat transfer coefficient and T_S the soil tempera-ture. Equation (1) is completed by initial conditions $p(x, 0) = p_0(x)$ and $T(x, 0) = T_0(x)$ and boundary conditions $p(0, t) = p_0$, $T(0, t) = T_0$ and gas demand $\dot{m}(\grave{}, t)$ at the outlet of the pipeline with length $\grave{}$ (see Fig. 4).

The numerical approximation of the hyperbolic system of PDEs is carried out using the method of lines paradigm [27]. The spatial domain $[0, \grave{}]$ was uniformly discretized by n_x points. The system of ordinary differential equations (ODEs) can be written as

$$\frac{\mathrm{d}w(t)}{\mathrm{d}t} = -F(w)\mathrm{B}w(t) - S(w(t)) = f(w(t)), \quad w(t_0) = w_0, \quad t \in [0, t_f], \tag{8}$$

where state vector $w(t) = [p_1(t), \cdots, p_i(t), \cdots, p_{n_x}(t), \dot{m}_1(t), \cdots, \dot{m}_i(t), \cdots, \dot{m}_{n_x}(t), T_1(t), \cdots, T_i(t), \cdots, T_{n_x}(t)]^{>}$, t_f is the total simulation time, and $\mathrm{B} = \sum_{j=1}^{n} I_j \otimes \mathrm{B}^{(j)}$ which refers to the computational stencil. The latter is the Kronecker product of $\mathrm{B}^{(j)}$ and identity matrix I_j. A central difference scheme of the second order is used whereas the weighting coefficients in $\mathrm{B}^{(j)}$ are defined as [27]

$$\frac{1}{2\Delta^{x}} \begin{matrix} -34-1 \\ -1 \quad 0 \quad 1 \\ 1 \quad 4 \quad 3 \end{matrix}, \tag{9}$$

where Δx is the spatial step size.

Within the particle filter framework, the ODEs are solved many times with the use an ensemble N_p of realizations of the system state to represent

probability distributions. In [14], it was shown that for the time integration, the second-order diagonally implicit Runge–Kutta method is reliable and shows good accuracy and efficiency properties [12, 13]. Moreover, to reduce the computation time, the sparsity of the system is applied. If n_x = 101 is considered, then only 2.951% of the entries are nonzero.

3 Particle filtering

Within the framework of data assimilation, the optimal state of an evolv-ing physical system is sought through application of limited measurements. The prediction of the state is performed using the underlying deterministic gas flow equations in the presence of stochastic process, numerical errors and an incomplete description of the physical phenomenon. In contrast to Kalman filters, including its variants, Monte-Carlo techniques or particle filters are not constrained by linearity or Gaussianity. This ensemble-based data assimilation approach is characterized by efficient convergence properties that result from the law of large numbers and based on Bayes theorem proving that a model probability density function (pdf) can be updated via measurements. Mathematically it can be formulated as follows:

$$\zeta_k = g(\zeta_{k-1}) + v_{k-1}\,, \tag{10}$$

$$y_k = \zeta_k + n_k\,, \tag{11}$$

where $\zeta_k \in R^{n_\zeta}$ denotes the state variables at time k, $y_k \in R^{n_y}$ refers to the measurement data, $v_k \in R^{n_v}$ and $n_k \in R^{n_n}$ represent the model and measurement noise, respectively. The model noise parameters are in practice predefined but and often based on trial-and-error or tuning [15]. The discretized flow model is denoted by $g : R^{n_\zeta} \times R^{n_v} 7\rightarrow R^{n_\zeta}$. The state variables, which in this case are measured directly, contain noise and are sought to minimize an error by data assimilation. A well-known technique is particle filtering applied to approximate the posterior distribu-tion $\pi(\zeta_{0:k}|y_{1:k})$, where $\zeta_{0:k} = \{\zeta_0, \zeta_1, \ldots, \zeta_k\}$ and $y_{1:k} = \{y_1, y_2, \ldots, y_k\}$. Particle filters find a set of states $\zeta_{0:k}$ in time k through updating a random measure $\zeta_{0:k}^{i}, \omega_k^{i}\,{}_{i=1}^{N_p}$ that approximates $\pi(\zeta_{0:k}|y_{1:k})$ where $\{\zeta_{0:k}^{i}, i = 0, \ldots, N_p\}$ is a set of support points and $\{\omega_k^{i}, i = 1, \ldots, N_p\}$ are associ-ated weights. In general this technique starts with sampling N_p particles ζ_0^{i} from the initial model probability density $\pi(\zeta_0)$ followed by integrating all particles in time up to the moment measurements become available, i.e. $\zeta_k^{i} \sim \pi(\zeta_k|\zeta_k^{i}{}_{-1})\forall i$. Here the importance density $\pi(\zeta_k|\zeta_k^{i}{}_{-1}, y_k)$ is set equal

to the prior $\pi(\zeta_k|\zeta_k^{j}{}_{-1})$. The weights $\omega_k^{j} = \pi(y_k|\zeta_k^{j})$ N_p

X

puted followed by a resampling step of the particles in such a manner that the weights are equal to N_p^{-1}. The resampling step is repeated for all measurements. The resampling step excludes particles with low weights and maintain particles with high weights for the posterior probability density function. Details related to the particle filter can be found in [6–8]. Particle filters might show a drawback of dimensionality, namely that the ensemble size to generate a few samples from the high-probability areas of the posterior is growing exponentially with the dimension of the state vector [16, 17]. In this work, a coarse interval is used, whereas the sampling is carried out only at the inlet and the outlet node. As a result, it can be assumed that the drawback of dimensionality will not be an issue.

4 Strength of defected tube

The Det Norske Veritas recommended practice methodology was selected, as it is considered adequate for electrochemical corrosion defects and a steel grade investigated in this study [18]. The maximum allowable operating pressure of the defected pipeline with a longitudinally oriented single metal loss (see Fig. 1) is defined in [18]:

$$MAOP_{\mathrm{DNV}} = \gamma_m \frac{2\delta f_u \left(1 - \gamma_d \frac{d}{\delta_*}\right)}{\gamma_d \left(o - \frac{d}{Q}\right)}, \tag{12}$$

where

$$\frac{d}{\delta_*} = \frac{\frac{d}{\delta}_{\mathrm{means}} + \varepsilon_d \mathrm{SD}\left(\frac{d}{\delta}\right)}{L^2}, \tag{13}$$

where: D_o – outside diameter, f_u – ultimate tensile strength of the pipe steel applied in the design, d – single defect depth derived from diagnos-tics, L – defect length derived from the in-line inspection, δ – wall nominal

thickness, $(d/\delta)_{means}$ – measured (relative) single defect depth obtained from the inspection results, and SD(d/δ) – standard deviation of the measured ratio derived from the specification of MFL tool by the assumption of normal distribution of random variable d/δ [18].

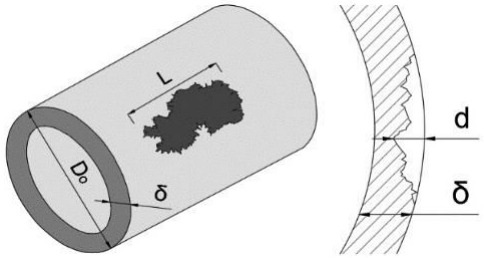

Figure 1: Geometry of the axially oriented tube wall material loss [22].

The safety factors γ_m, γ_d, and ε_d in Eqs. (12), (13) and are determined by (i) pipeline safety class, usually derived from the design, (ii) testing method, relative or absolute, and (iii) inspection accuracy and a confidence level. According to Polish regulation, the degree of area urbanization concerning the location of high-pressure gas pipelines is classified as follows:

- Class 1 (safety class high corresponding to the pipeline segment design factor $f \leq 0.4$) covers an area built over with single- or multi-family collective dwelling houses and public utility facilities, with intensive vehicular traffic and developed underground infrastructure.
- Class 2 (safety class normal corresponding to the pipeline segment design factor $0.4 < f \leq 0.6$) comprises an area with single-family and farmstead housing and individual leisure buildings along with their necessary infrastructure.
- Class 3 (safety class low corresponding to the pipeline segment design factor $0.6 < f \leq 0.72$) includes an undeveloped area and an area in which only isolated single-family houses, farms and livestock buildings, along with their necessary infrastructure, can be situated.

The safety factor γ_m is obtained from in-line inspections based on relative feature depth measurements such as the MFL method. The value of the factor is $\gamma_m = 0.70$ for Class 3. The partial safety factor for corrosion depth is $\gamma_d = 1.16$. The fractile value for corrosion $\varepsilon_d = 0\ 0$. The two latter factors depend on the safety class and standard deviation and are selected according to [18].

5 Strength of multi-layer composite flexible wrap

The components of a layered system applied to repair a steel pipe with a volumetric defect in the present research as well as in [3, 20, 22] are shown in Fig. 2. The pipe is wrapped with concentric layers of either a fibreglass or a carbon fibre with epoxy resin.

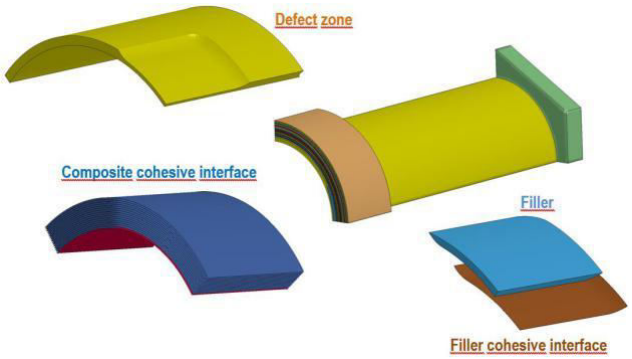

Figure 2: Layered system of the composite repair used for reinforcement of a steel pipe with a metal loss [22].

Evidently, the strength of steel pipes reinforced with a composite repair depends on material properties of the sleeve components and the number of layers applied. Figure 3 shows the von Mises stress – pressure curve for a different number of inference layers for the case studied in [20]. The results were obtained from finite element method computations for a machined defected steel tube diameter of 0.219 m and wall thickness of 0.006 m repaired with the flexible fibreglass with epoxy resin wraps. While applying a composite sleeve, a significant increase in pipeline strength, exceeding the value for the intact tube, is observed. An increase in the internal pressure causes fibre breakage and, as a consequence, burst of the steel pipe parallel to the pipe axis. The calculations showed that if the number of layers increases, the rupture pressure of defective pipe increases as well. However, starting from 16 composite layers, a change in the burst pressure is relatively small. Numerical simulations conducted for the considered case showed that the maximum pressure until fracture reaches is 38.5 MPa for 40 layers of fibreglass.

The strength calculations applied in the present paper are applicable for estimating the failure pressure of a corroded pipe reinforced with a multi-layer composite wrap. Assuming the elastic behavior of both the steel tube

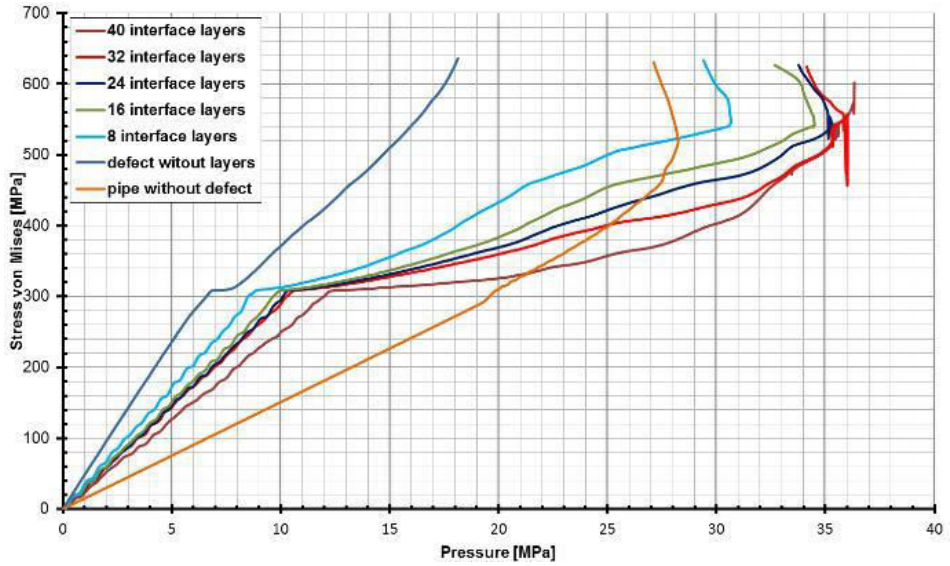

Figure 3: Influence of the number of layers on the stress-pressure curve.

and the sleeve, the rupture pressure of a straight pipe, considered as a thin-walled shell with volumetric surface defect reinforced with a flexible wrap, can be calculated as follows [3, 19, 23]:

$$p_{\max}^{th} = \frac{f_u (r_o - r_i)}{\alpha_\theta (r_i - \eta r_o)}, \tag{14}$$

where

$$\alpha_\theta = \frac{1 - \frac{d}{\delta}\frac{1}{Q}}{1 - \frac{d}{\delta}}, \tag{15}$$

$$\eta = \frac{r_i^2 E_{pipe} (r_o - r_i)}{r_i^2 E_{sleeve} (r_e - r_o)} + \frac{r_o}{r_i}\left(\frac{r_o}{r_i}\right)^{-1}, \tag{16}$$

where: p^{th}_{max} – failure pressure of a straight pipe with a volumetric defect reinforced a composite wrap, r_e – external radius of the steel tube plus thickness of the sleeve, r_i – inner radius of the steel pipe, r_o – external radius of the steel pipe, E_{pipe} – elasticity modulus of steel and E_{sleeve} – elasticity modulus in the circumferential direction of the composite sleeve material.

The elasticity modulus of a sleeve depends on the components material properties of the layered system used for the pipeline reinforcement. However, the elasticity modulus of the composite sleeve depends on the fibre volume as well. Analyses of defective-pipe reinforcement systems confirm the assumption that an averaged elasticity modulus of the material in the hoop direction is approximately equal to a mean of an axial and a transverse value of the fibre and the resin. These assumptions were applied in [3, 19]. According to [23], the average elasticity modules in the circumferential direction of the fibreglass sleeve can be assumed as 25 GPa. This composite is a commercial product, called Syntho-Glass XT, from Neptune Research Inc. According to [24], the average elasticity modulus in the circumferential direction of the carbon-based wrap can be assumed as 85 GPa. This laminate, called Steel-Wrap E, is a commercial product from NRI. The tension elasticity modules used in this work are shown in Table 1.

Table 1: Elasticity modulus of steel, fibreglass sleeve and epoxy filler used in the study.

Elasticity modulus of steel, E_{pipe} [GPa]	Average circumferential modulus of fibreglass sleeve, E_{pipe} [GPa]	Average circumferential modulus of carbon fibre sleeve, E_{pipe} [GPa]	Average modulus of epoxy resin, E_R [GPa]
206.0	25.0	85.0	5.5

The acceptability condition of tube wall metal loss without reinforcement can be written as follows:

$$p(x)_{est} \leq MAOP_{DNV}, \tag{17}$$

where: $p(x)_{est}$ – pressure estimated from the flow model at the metal loss coordinate x along the pipeline, $MAOP_{DNV}$ – maximum allowable oper-ating pressure of the defected thin-walled cylinder with a longitudinally oriented single metal loss calculated according to [18]. The thickness of the multi-layer composite sleeve ($k = r_e - r_o$, where r_e is the external radius of the pipe with sleeve, r_e is the external radius of the pipe) needs to be deter-mined in order to reach the minimum strength of the reinforced tube. The condition for the maximum admissible operating pressure of the pipeline with a volumetric surface flaw reinforced with the composite laminate can be expressed by:

$$MAOP^{th} \leq f\, p_{max}{}^{th}, \tag{18}$$

where: $f = 0.72$ – design factor usually applied in gas transmission design and $MAOP^{th}$ – maximum admissible operating pressure of the thin-walled

cylinder containing a volumetric surface defect reinforced with a multi-layer composite sleeve.

The safety factor 0.72 is usually related to the yield stress in many pipeline design codes. However, the ultimate strength is a material prop-erty responsible for the fracture of the intact steel pipe. The problem of transition between the safety factors adopted in the design codes and fit-ness for service standards exists and is well known. The approach based on the steel ultimate tensile strength of in-service pipelines, applied in the present paper as well as in [21], is less conservative compared to other ap-proaches based on the yield stress. It results from a value of a ratio between the ultimate tensile strength and the yield strength within the scope of 1.1, for high strength steels, and 1.7 for low strength construction steels which are ductile in a wider range. It means that the fracture pressure, based on the ultimate tensile strength applied in Eq. (15) and corresponding formula (19), is 18% higher for the considered steel grade L 485 ME (X70).

To resist the estimated pressure dynamics in the pipeline, at the defect location, the following inequality needs to be satisfied for every repaired part-wall metal loss reinforced with a composite sleeve:

$$p(x)_{\mathrm{est}} \le MAOP^{\mathrm{th}} \le f\, p_{\max}{}^{\mathrm{th}} . \tag{19}$$

Based on in-line inspection results, in which pipe wall metal losses were identified, it was inferred that conditions (19) and (20) need to be fulfilled for each volumetric surface defect on the pipeline.

6 Case study

In this section, the flow dynamics is estimated using the particle filter. As a result, the maximum pressure is obtained at the defect location in the time and spatial domain. Next, the internal fluid pressure is compared with the maximum allowable operating pressure of the tube with part-wall metal loss. The results enable analyzing the strength of the defected pipe, reinforced with fibreglass sleeve, in particular, to evaluate the appropriate thickness of a multi-layered repair wrap.

6.1 Maximum pressure estimates

For the analysis, a section of the Yamal transit pipeline on Polish territory was selected. The buried pipeline is characterized by the following parame-ters: ` = 177 km, D_i = 1.380 m and ε = 0.0015 mm. The soil parameters are

set as follows: T_S = 285.15 K and U = 1.66 W/m^2·K. The mean molar composition of natural gas is: 98.3455 CH_4, 0.6104 C_2H_6, 0.1572 C_3H_8, 0.0299 *i*-C_4H_{10}, 0.0253 *n*-C_4H_{10}, 0.0055 *i*-C_5H_{12}, 0.0040 *n*–C_5H_{12}, 0.0303 N_2 and 0.7918 CO_2. The Groupe Européen de Recherches Gazières (GERG) 2008 multi-parameter equation of state (EOS) is used to determine indirectly the thermodynamic and transport properties [29]. This equation of state is very accurate but computationally expensive and therefore less practical for pipeline simulations. Nevertheless, to benefit from its high accuracy, the properties were fitted to a multivariate regression model, that is,

$$\kappa(p, T) = \sum_{i=1}^{n} \imath_i p^{\mathrm{I}_{i,1}} T^{\mathrm{I}_{i,2}}, \quad 0.1\ \text{MPa} \le p \le 10\ \text{MPa}, \quad 253.15\ \text{K} \le T \le 313.15\ \text{K}, \tag{20}$$

where I as the power and $\imath_i$ refers to the corresponding coefficients and assumed is 5 degrees freedom. The average absolute deviation for all prop-erties is below 0.11%. The regression model is valid only within the pressure and temperature range for the given gas composition.

The simulations were done on the domain t_f = 0−24 h with $p(0, t)$ = 8.4 MPa, $T(0, t)$ = 308.15 K and $\dot{m}(\grave{}, t)$ is shown in Fig. 4.

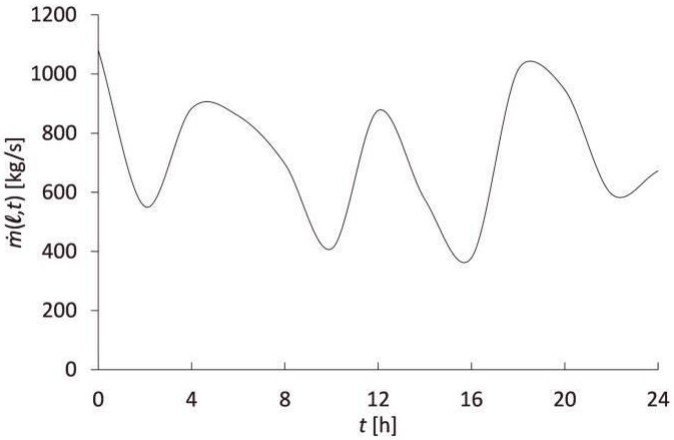

Figure 4: Mass flow rate boundary condition.

In data assimilation, a common practice is to use synthetic data in the absence of the real data. However, it is important to avoid the in-

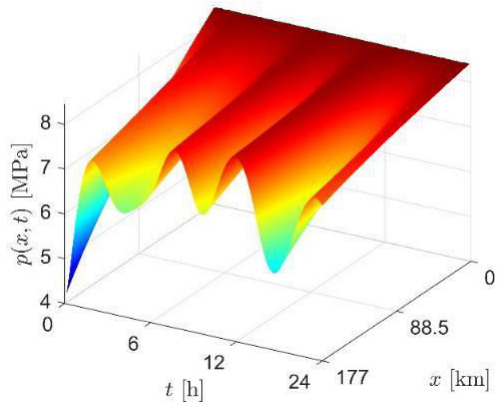

(a)

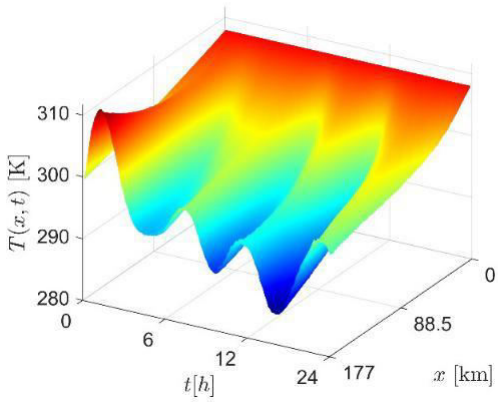

(b)

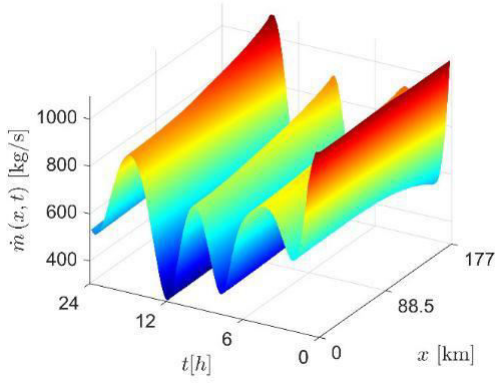

(c)

Figure 5: Temporal and spatial evolution of estimates using the particle filter with $v_{k-1} \sim (\alpha, \beta)$: a) pressure, b) temperature, c) mass flow rate.

verse crime [28], that is, the numerical model is solved on a coarser grid than the one used to generate the data, otherwise too optimistic estimates might be obtained. In this work, the measurement data was generated by adding random Gaussian noise to the fine grid solutions of pressure, temper-ature and mass flow rate, that is $n_{k,p} \sim \mathrm{N}\ 0,\ 0.04^2$, $n_{k,T} \sim \mathrm{N}\ 0,\ 1.5^2$ and $n_{k,\dot{m}} \sim \mathrm{N}\ 0,\ 2.5^2$ with variance in MPa^2, K^2, and $(\mathrm{kg/s})^2$, respectively. For the description of the model noise randomness is drawn from the gamma distribution $v_{k-1} \sim (\alpha,\ \beta)$, whereas for each state variable it is specified as follows: $v_{k-1,p} \sim (9,\ 0.5)$, $v_{k-1,T} \sim (5,\ 1)$ and $v_{k-1,\dot{m}} \sim (3,\ 2)$. A sen-sitivity analysis is conducted by increasing and decreasing the parameters by 20%. The random variables were generated using Matlab functions randn and gamrnd [30]. The particle size N_p is set to 50 and the sampling time of the measurements is 10 min. In practice, the sampling rate can vary from one to several tens of minutes. The evolution of the state variables is shown in Fig. 5. It is assumed that the location of the part-wall volumetric defect is located 21 km from the up-stream compressor station. In practice, this information is obtained from MFL diagnostics. Figure 6 shows the pressure variation as a function of time at the defect location. The maximum values for different noise parameters are shown in Table 2.

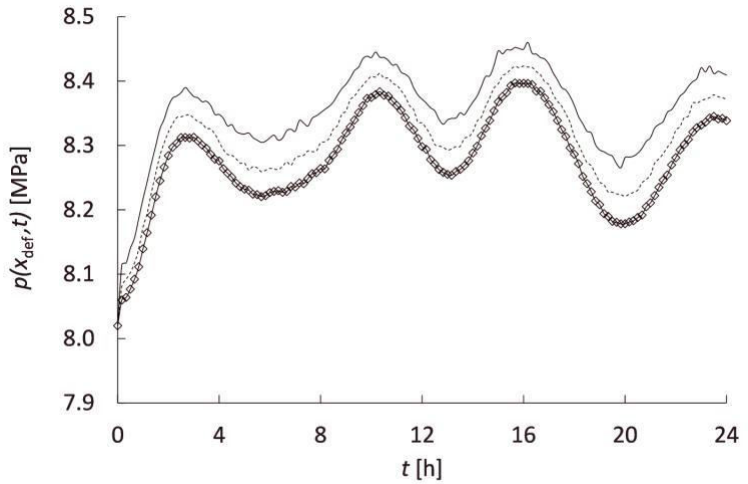

Figure 6: Pressure conditions at the volumetric defect location x = 21 km for different parameters of gamma distribution. – – – $v_{k-1} \sim (\alpha,\ \beta)$, — $v_{k-1} \sim$ $(1.2 \cdot (\alpha,\ \beta))$ and — ♦ — $v_{k-1} \sim$ $(0.8 \cdot (\alpha,\ \beta))$.

Table 2: Maximum pressure at defect location for different parameters of the gamma distribution, $v_{k-1} \sim (\alpha, \beta)$.

Parameters	$p(21)_{est}$ [MPa]	$t_{max,p}$ [h]
$0.8 \cdot (\alpha, \beta)$	8.397	15.67
(α, β)	8.423	16.00
$1.2 \cdot (\alpha, \beta)$	8.460	16.17

6.2 Strength of the repaired steel tube by the composite sleeve

In the second part of this case study, the allowable pressure is calcu-lated based on the following L485MB steel grade pipeline parameters [22]: f_u = 570.0 MPa, f_y = 485 MPa, E_{pipe} = 206 GPa, D_o = 1.422 m, δ = 0.021 m, r_o = 0.711 m and r_i = 0.690 m. Dimensions of the longitudi-nally oriented corrosion area are obtained from a hypothetical in-line in-spection and shown in Fig. 1. Based on MFL diagnostics data, the maxi-mum defect depth, as a percentage of the nominal tube wall thickness, is $(d/\delta)_{means}$ = 43% and the axial length L of the corroded area is 1000 mm.

The maximum allowable operating pressure of the defected pipe with-out reinforcement calculated from Eqs. (12)–(14) equals to $MAOP_{DNV}$ = 7.98 MPa. The maximum estimated pressure $p(21)_{est}$ obtained from the data assimilation approach at the defect location on 21 km on the pipeline, for different parameters of the gamma distribution specified in Table 2, shows higher values than $MAOP_{DNV}$. This means that condition (18) is not fulfilled and therefore the pipeline must be immediately excavated, and the defect needs to be directly assessed as described in [2]. If the in-line inspection tool defect indication is confirmed, the volumetric metal loss feature needs to be reinforced with a composite wrap in order to reach the minimum required strength of the tube. The required number of sleeve lay-ers k for two kinds of materials for different gas pressures obtained from data assimilation is shown in Table 3.

For the number of layers of the fibreglass wrap k = 30, the corre-sponding burst pressure of the repaired tube equals to p^{th}_{max} = 11.637 MPa. From Eq. (19), the maximum admissible operating pressure of the pipeline containing a volumetric surface defect reinforced with a Syntho-Glass XT composite sleeve equals to $MAOP^{th}$ = 8.402 MPa with k = 32. However, for the specific defect dimensions taken into consideration, the number of layers of carbon fibre composite sleeve obtained from Eqs. (15)–(19) equals

Table 3: Different composite materials to repair the pipe considering the transient fluid pressure at the defect location.

$p(21)_{est}$ [MPa]	$MAOP^{th}$ [MPa]	Number of layers k/ Composite material
8.397	8.402	32 / fibreglass
8.397	8.417	10 / carbon fibre
8.423	8.424	35 / fibreglass
8.423	8.441	11 / carbon fibre
8.460	8.461	40 / fibreglass
8.460	8.460	12 / carbon fibre

to k = 10, in order to fulfill condition (20). It means that applying carbon fibre reinforcement, the number of layers significantly decreases, as shown in Table 3. This is due to the elasticity modulus of carbon-based material which is 3.5 times higher than fibreglass.

7 Conclusions

An ensemble-based data assimilation technique was applied to estimate the pressure under transient flow conditions at the point where a tube part-wall defect exists in order to evaluate the gas transmission pipeline strength. This approach is more accurate and realistic compared to a situ-ation where the pressure does not change in time, which is usually assumed in thin-walled tubes strength analysis during operation. The pipe struc-tural integrity was examined for different commercially available composite materials and noise statistics in the unsteady pressure-flow model. The strength computations applied in the current present paper are a good ap-proximation to estimate the failure pressure of corroded tubes reinforced with sleeves subjected to the pressure variation in the pipeline. Repairs with the use of composite sleeves of part-wall surface metal losses derived from a periodic in-line inspection of an underground structure avoid un-necessary capacity limitations of steel network subjected to corrosion, due to local reinforcement of the pipe in order to maintain design-operating pressure of the infrastructure.

Acknowledgements The authors wish to thank anonymous Reviewers whose valuable comments and suggestions helped to improve the content of this paper.

Received 26 April 2020

References

[1] Bouledroua O., Zelmati D., Hassai M.: *Inspections, statistical and reliability assessment study of corroded pipeline*. Eng. Fail. Anal. **100**(2019), 1–10.

[2] Witek M.: *Life cycle estimation of high pressure pipeline based on in-line inspection data*, Eng. Fail. Anal. **104**(2019), 255–272.

[3] Witek M.: *Gas transmission failure probability estimation and defect repairs activities based on in-line inspection data*. Eng. Fail. Anal. **70**(2016), 255–272.

[4] Siraj T.: *Quantification of Uncertainties in Inline Inspection Data for Metal-loss Corrosion on Energy Pipelines and Implications for Reliability Analysis*. PhD thesis, University of Western Ontario, London 2018.

[5] Witek M., Batura A., Orynyak I., Borodii M.: *An integrated risk assessment of onshore gas transmission pipelines based on defect population*. Eng. Struct. **173**(2018), 150–165.

[6] Arulampam S., Maskell S., Gordon N., Clapp T.: *A tutorial on particle filters for online non-linear/non-Gaussian Bayesian tracking*. IEEE T. Signal Proces. **50**(2002), 2, 174.

[7] Doucet A.: *On sequential Monte Carlo methods for Bayesian filtering. Tech. rep.* Tech. Rep., Univ. Cambridge, Depart. Eng., Cambridge 1998.

[8] Gordon N., Salmond D., Smith A.: *Novel approach to nonlinear/non-Gaussian Bayesian state estimation*. IEE Proc. F – Radar Signal Process. **140**(1993), 2, 107–113.

[9] Han Z.Y., Weng W.G.: *An integrated quantitative risk analysis method for natural gas pipeline network*. J. Loss Prevent. Proc. **23**(2010), 428–436.

[10] Uilhoorn F.E.: *Comparison of Bayesian estimation methods for modeling flow transients in gas pipelines*. J. Nat. Gas Sci. Eng. **38**(2017), 159–170.

[11] Colebrook C.: *Turbulent flow in pipes, with particular reference to the transition region between the smooth and rough pipe laws*. J. Inst. Civil Eng. **11**(1939), 133–156.

[12] Bank R.E., Coughran, Jr. W.M., Fichtner W., Grosse E.H., Rose D.J., Smith R.K.: *Transient simulation of silicon devices and circuits*. IEEE T. Comput. Aid. D. CAD **4**(1985), 4, 436–451.

[13] Shampine L., Hosea M.: *Analysis and implementation of TR-BDF2*. Appl. Numer. Math. **20**(1996), 1–2, 21–37.

[14] Uilhoorn F.E.: *A comparison of numerical integration schemes for particle filter-based estimation of gas flow dynamics*. Phys. Scripta **93**(2018), 12.

[15] Uilhoorn F.E.: *A multiobjective optimization approach to filter tuning applied to coupled hyperbolic PDEs describing gas flow dynamics*. Optimal Control Appl. Meth. **40**(2019), 4, 750–763.

[16] Bickel P., Li B., Bengtsson T.: *Sharp failure rates for the bootstrap particle filter in high dimensions*. In: IMS Collections, Vol. 3, Pushing the Limits of Contemporary Statistics: Contributions in Honor of Jayanta K. Ghosh (B. Clarke, S. Ghosa, Eds.). IMS, Beachwood 2018, 318–329.

[17] Snyder C., Bengtsson T., Bickel T., Anderson J.: *Obstacles to high-dimensional particle filtering*. Mon. Weather Rev. **136**(2008), 4629–4640.

[18] Det Norske Veritas: *Recommended practice DNV-RP-F101. Corroded pipelines*. 2010.

[19] Da Costa Mattos H.S., Reis J.M.L, Paim L.M., Silva da M.L., Lopes Jr. R., Perrut V.A.: *Failure analysis of corroded pipelines reinforced with composite repair systems*. Eng. Fail. Anal. **59**(2016), 223–236.

[20] Mazurkiewicz Ł., Tomaszewski M., Małachowski J., Sybilski K., Chebakov M., Witek M., Yukhymets P., Dmitrienko R.: *Experimental and numerical study of steel pipe with part-wall defect reinforced with fibre glass sleeve*. Int. J. Pres. Ves. Pip. **149**(2017), 108–119.

[21] Orynyak I.V.: *Leak and break models of ductile fracture of pressurized pipe with axial defects*. In: Proc. 6th Int. Pipeline Conf. (IPC2006), Sept. 25–29, 2006, Calgary, IPC206-10066

[22] Uilhoorn F., Witek M.: *Influence of unsteady pressure-flow conditions on strength of steel pipelines with volumetric defects reinforced by composite sleeves*. In: XIV Research and Development in Power Engineering Conf. (RDPE 2019), Warsaw, Dec. 3–6, 2019.

[23] Reis J.M.L., Chaves F.L., Da Costa Mattos H.S.: *Tensile behaviour of glass fibre reinforced polyurethane at different strain rates*. Mater. Des. **49**(2013), 192–196.

[24] Alizadeh E., Dehestani M.: *Analytical and numerical fracture analysis of pressure vessel containing wall crack and reinforcement with CFRP laminates*. Thin-Wall. Struct. **127**(2018), 210–220.

[25] Aleksander C., Ochoa O.O.: *Extending onshore pipeline repair to offshore steel risers with carbon–fiber reinforced composites*. Compos. Struct. **92**(2010), 499–507.

[26] Lim K.S., Azraai S.N.A., Yahaya N. Noor M.N., Zardasti L., Kim J.-H.J.: *Behaviour of steel pipelines with composite repairs analysed using experimental and numerical approaches*. Thin-Wall. Struct. **139**(2019), 321–333.

[27] Schiesser W.E.: *The Numerical Method of Lines: Integration of Partial Differential Equations*, Academic Press, San Diego 1991.

[28] Kaipio J., Somersalo E.: *Statistical and Computational Inverse Problems. Applied Mathematical Sciences*. Springer-Verlag, New York 2005.

[29] Kunz O., Wagner W. J.: *The GERG-2008 wide-range equation of state for natural gases and other mixtures: An expansion of GERG-2004*. Chem. Eng. Data **57**(2012), 3032–3091.

[30] MATLAB. version 9.7.0.1261785 (R2019b). Natick, Massachusetts: The MathWorks Inc.